

# Thickness Variation of a Thin Film under the Influence of External Forces

C. V. TU and W. Y. D. YUEN

Research & Technology Centre, BHP Coated Products Division.

## ABSTRACT

In continuous strip coating processes, a thin film is normally applied onto the strip by a roller coating or dipping process. Due to the three-dimensional effects near the strip edges, the coating at these regions is often thicker than the rest, causing undesirable effects such as 'cotton reeling' during recoiling. Edge devices are often used to produce favourable force distribution near the strip edges to remove the excess coating.

This paper presents an analysis of the fluid flow in the vicinity of the strip edges under the influence of external forces, with the transient variation of the coating thickness deduced. The solution has been used to examine the operating characteristics of the edge devices for the hot dip galvanizing process with the final coating thickness distribution predicted.

## INTRODUCTION

In most applications, metal strip is coated with a thin film of protective layer for added corrosion resistance and surface appearance. The protective layer is commonly applied, in liquid form, by a roller coating process or by a hot dipping method. In these continuous processes, the prime considerations in quality control are the surface appearance, coating thickness and its uniformity in distribution. However, because of the three-dimensional effects near the strip edges during the application of the coating, the film thickness near these regions requires additional control if a thicker coating, also known as edge build-up (as shown in Figure 1a), is to be avoided. Otherwise, the thicker edge could cause various problems such as 'cotton reeling' during recoiling, and edge flaking during forming.

The edge build-up defect can be minimized by devices such as 'edge baffles' or 'false edges' which may be classified as passive devices since no external energy is required in their application. Although these devices are sufficiently effective in many applications, the use of an active device, which induces suitable surface forces on the coating, can be advantageous because it offers a wider scope in controlling the edge coating thickness.

This paper presents an analysis of the fluid flow of an incompressible film under the influence of external forces. The solution is then applied to examine the operational characteristics of an active edge device in controlling the coating thickness near the strip edges.

## ANALYSIS

Consider a film of viscous incompressible fluid on a substrate with an initial film thickness  $h(x)$ , which is taken to vary slowly with the horizontal dimension  $x$  as shown in Figure 1b (ie  $|dh/dx| \ll 1$ ).

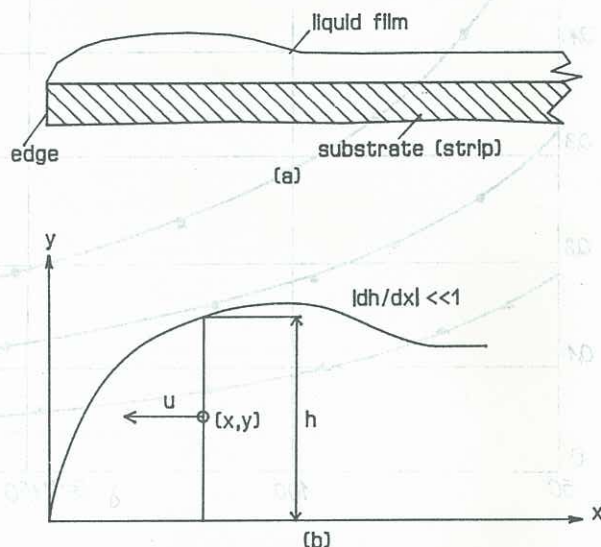


Figure 1 (a) Build-up near the strip edge;  
(b) co-ordinate system employed.

The film is assumed to be under the influence of external forces produced by a pressure gradient and a surface shear stress field acting in the  $x$ -direction only. The Navier Stokes equations for a thin film on a plane surface reduce to:

$$\rho(\partial u / \partial t) = \mu(\partial^2 u / \partial y^2) - G \quad (1)$$

$$\text{where } G = (\partial p / \partial x) - \sigma(\partial^3 h / \partial x^3) \quad (2)$$

Here  $u \equiv u(y, t)$  is the velocity component along the  $x$ -direction as shown in Figure 1b,  $\rho$ ,  $\sigma$  and  $\mu$  are the density, surface tension and viscosity of the coating fluid respectively,  $\partial p / \partial x$  is the pressure gradient (which varies slowly with parameters other than the  $x$  dimension), and  $t$  the time.

The boundary conditions for an initially stationary film (in the  $x$ -direction), no slip at the film-substrate interface, and a free surface are, respectively,

$$u(y, 0) = 0 \quad (3)$$

$$u(0, t) = 0 \quad (4)$$

$$\text{and } \partial u(h, t) / \partial y = \tau / \mu \quad (5)$$

where  $\tau(x)$  is the external shear stress applied onto the film surface.

Equation (1), with the above boundary conditions, may be solved using a Laplace transformation, and a series solution for short-time is obtained:



$$u = (4Gt/\rho) \sum_{n=0}^{\infty} \{(-1)^n [f_2(n+1, -\frac{1}{2}) + f_2(n, \frac{1}{2})] + [2\tau(vt)^{\frac{1}{2}}/\mu] x \sum_{n=0}^{\infty} \{(-1)^n [f_1(n+\frac{1}{2}, -\frac{1}{2}) - f_1(n+\frac{1}{2}, \frac{1}{2})] - Gt/\rho \} \quad (6)$$

$$\text{where } f_m(r, s) = i^m \operatorname{erfc}[(rh+sy)/(vt)^{\frac{1}{2}}]$$

and  $\nu = \mu/\rho$  is the kinematic viscosity.

In addition, conservation of mass requires

$$\partial h/\partial t = -\partial(\int_0^h u dy)/\partial x \quad (7)$$

which, on substitution of Equation (6) and after simplifications, reduces to

$$\partial h/\partial t = F_1 + F_2 + F_3 \quad (8)$$

where

$$F_1 = -[8t(vt)^{\frac{1}{2}}/\rho] \{G' \sum_{n=1}^{\infty} [(-1)^n \{2f_3(n, 0) + 1/(6\pi^{\frac{1}{2}})\}] - G \sum_{n=1}^{\infty} [(-1)^n \{2n/(vt)^{\frac{1}{2}}\} (\partial h/\partial x) f_2(n, 0)] \} \quad (9)$$

$$F_2 = -(4t/\rho) \{(\partial \tau/\partial x) [\sum_{n=0}^{\infty} \{2(-1)^n f_2(n+\frac{1}{2}, 0)\}] + \tau \sum_{n=1}^{\infty} [(-1)^n \{(2n+1)/(vt)^{\frac{1}{2}}\} (\partial h/\partial x) f_1(n+\frac{1}{2}, 0)] \} \quad (10)$$

$$F_3 = G'th/\rho + (Gt/\rho) (\partial h/\partial x) \quad (11)$$

$$G' = \partial G/\partial x \quad (12)$$

Given the initial coating thickness, pressure gradient and surface shear stress distributions, the transient film thickness distribution,  $h(x, t)$ , can be computed numerically from Equation (8).

The solution of Equation (6) is applicable when the elapsed time is reasonably short. Another series solution for long-time may be derived following a similar approach:

$$u = (2Gt/\rho) \sum_{n=0}^{\infty} \{(\frac{1}{2})^n x \sum_{k=0}^n [(\frac{n}{k}) (-1)^k \{f_2(k, \frac{1}{2}) + f_2(k+1, -\frac{1}{2})\}] - Gt/\rho + [\tau(vt)^{\frac{1}{2}}/\mu] \sum_{n=0}^{\infty} \{(\frac{1}{2})^n x \sum_{k=0}^n [(\frac{n}{k}) (-1)^k \{f_1(k+\frac{1}{2}, -\frac{1}{2}) - f_1(k+\frac{1}{2}, \frac{1}{2})\}]\} \quad (13)$$

Using, again, the conservation of mass condition (Equation (7)), an expression similar to that of Equation (8) for  $\partial h/\partial t$  can be deduced.

If the inertia term in Equation (1) is neglected and the surface tension effect is insignificant, the above solution degenerates to

$$u = \frac{1}{2}(G/\mu)(y^2 - 2hy) + \tau y/\mu \quad (14)$$

$$\partial h/\partial t = (1/\mu) \partial(\frac{1}{2}Gh^3 - \frac{1}{2}\tau h^2)/\partial x \quad (15)$$

Here  $G = \partial p/\partial x$ .

#### APPLICATIONS

The above solution is now applied to examine the film flow near an edge of a strip under the influence of a pressure gradient and a surface shear stress field induced by a suction device.

##### Edge suction device

The external forces on the film surface are usually generated by an air-driven device positioned near the strip edge to create a region of low pressure at its entrance such that an air stream is induced across the surface of the coated strip edge as illustrated in Figure 2. Although, in general, the cross-section of the suction device can be of any practical shape, a simple circular section is used in this application with the suction induced by the ejector principle using compressed air.

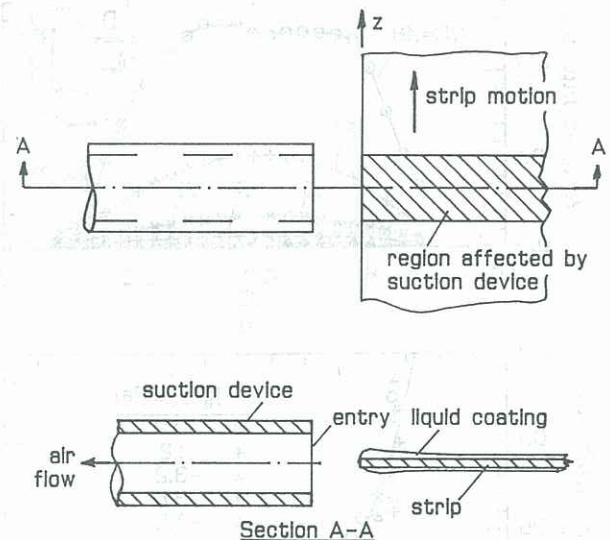


Figure 2 Location of the suction device with respect to the strip edge.

Since the coating thickness is usually much smaller than the other dimensions, its presence has insignificant influence on the surface static pressure,  $p_s$ , and the shear stress,  $\tau$ , induced by the suction device. Hence,  $p_s$  and  $\tau$  may be measured in the absence of the liquid film.

The pressures and shear stresses on the surface of a 5 mm thick acrylic plate (to simulate the strip) induced by a suction tube of 24 mm entry diameter were measured. The plate, which can be traversed in the vertical direction, consists of an array of pressure tappings connected to a multiplexer via embedded channels within the plate. Static pressures were measured using the Bell & Howell pressure transducers. The surface shear stresses were measured using Preston tubes (according to Patel's calibrations (Patel, 1965)) of diameters ranging from 0.42 to 0.65 mm. The shear stress measurements were then repeated using Stanton probes (Pai and Whitelaw, 1969) with a 'razor blade height' of 0.05 mm and a hole diameter of 0.70 mm, and good agreements were obtained.

The static pressure distribution on the plate, with its edge positioned at a fixed distance (2 mm) from the entry of the suction device, is plotted in Figure 3a, which indicates that the pressure distribution is fairly uniform in the direction along the strip movement and the influence of the suction device appears to be confined within a region corresponding to the internal diameter of the tube near its entry. It is therefore justifiable to assume that the pressure and surface shear stress variations are confined within the region shown in Figure 2, and that the pressure and shear stress distributions along the centre-line ( $z=0$ ) are applicable to other  $z$  co-ordinates within the affected region. Consequently, the solutions derived in the previous section are applicable.

The measured static pressures and surface shear stresses along the centre-line, non-dimensionalized by the suction tube entry pressure,  $p_e$ , are plotted in Figures 3b and 3c. It is observed that the effect of the distance of the plate from the suction tube is negligible, which is expected since the plate thickness is small compared to the tube diameter.

Simple expressions for  $p_s$  and  $\tau$  have been obtained by fitting the data of Figures 3b and 3c for  $x/D$  ranging from 0.2 to 1.0:



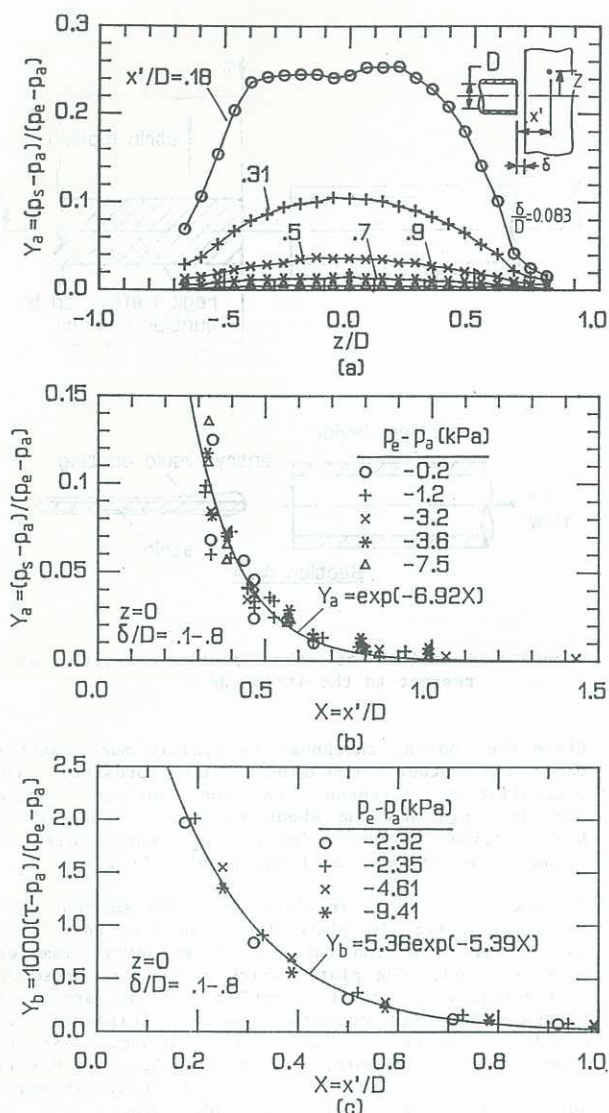


Figure 3 Measured (a) and (b) static pressure ( $p_s$ ), and (c) shear stress ( $\tau$ ) distributions on the plate surface ( $p_e$  = suction tube entry pressure,  $p_a$  = atmospheric pressure,  $D = 24$  mm).

$$(p_s - p_a) / (p_e - p_a) = e^{-ax'/D} \quad (16)$$

$$\text{and } (\tau - p_a) / (p_e - p_a) = be^{-cx'/D} \quad (17)$$

where  $D$  is the suction tube diameter,  $x'$  the distance from the suction tube entry (see Figure 3a),  $p_a$  the atmospheric pressure, and coefficients  $a$ ,  $b$  and  $c$  are found to be 6.92, 0.00536 and 5.39 respectively, with correlation coefficients of 0.947 and 0.993 calculated for  $p_s$  and  $\tau$  respectively.

#### Results and discussions

During the removal of the excess coating near the strip edge, the film is believed to behave in a manner as illustrated in Figure 4, with complicated formation of blobs which would eventually break off from the strip. However, the region of practical interest lies within the strip edges with the maximum edge coating thickness being the prime concern.

In order to apply the above analysis, the initial conditions, namely, the nominal film thickness and

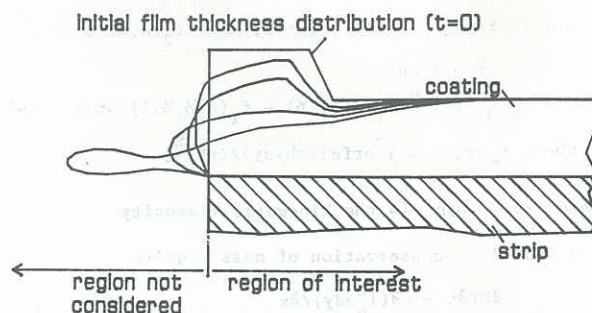


Figure 4 Qualitative illustration of the film flow under the influence of the suction device.

edge build-up profile, must be specified. The variation of the film thickness during the coating application has been studied by various workers, including Thornton and Graff (1976), Nikoleizig et al (1978) and Ellen and Tu (1984) for the jet stripping of the hot dipping process, and Savage (1982) for the roller coating process. The edge build-up profile induced during coating application and/or by the interaction of the stripping jets, however, has not been fully quantified although these have been discussed previously (eg Butler et al (1970), and Ellen and Tu (1983)). As an illustration, calculations were carried out for a strip with a liquid zinc coating of 25  $\mu\text{m}$  nominal thickness and an assumed edge film thickness of 30  $\mu\text{m}$  (over 5 mm), which reduces to the nominal value over 2 mm. The variation of the film thickness distribution with time, as the strip moves through the affected region of the suction device, is shown in Figures 5a and 5b. The final film thickness distribution is dependent on the elapsed time a fluid element travels under the influence of the external forces induced by the suction device, and hence is dependent on the strip speed and tube diameter. In these calculations, it is observed that the series solution of Equation (8) provides sufficient accuracy even when the elapsed time is long.

Results from the solution with the inertia term neglected (Equation (15)) are also plotted in Figure 5b (in dotted lines). It can be seen that, as expected, the film thicknesses calculated from the approximation solution are consistently smaller than those from the accurate solution. For the zinc coating being examined, the differences are insignificant. In addition, the surface tension effects are found to be negligible. Based on the same initial conditions, Figure 6 illustrates the variation of the film velocity,  $u$ , across its thickness at a distance of 4 mm from the strip edge for various time intervals. The velocity distribution is seen to approach that deduced from Equation (14) after an elapsed time of approximately 100 ms.

Despite the findings reported above, it must be cautioned that for coating with a higher density or for very high strip speed, the approximate solutions could become grossly inaccurate. In this case, the full solutions of Equations (6) and (8), or Equation (13), must be used.

In order to obtain a suitable design for a suction device, its operating characteristics must be understood, an important aspect of which is the elapsed time,  $t^*$ , required to reduce the maximum edge film thickness to the nominal value from a specified edge build-up profile. As an illustration, using the same edge build-up profile assumed above, Figure 7 gives the variation of  $t^*$  with the distance of the suction tube from the strip edge for various suction pressures,  $p_e$ . For other suction devices and/or edge build-up conditions, similar figures may be generated and the suction



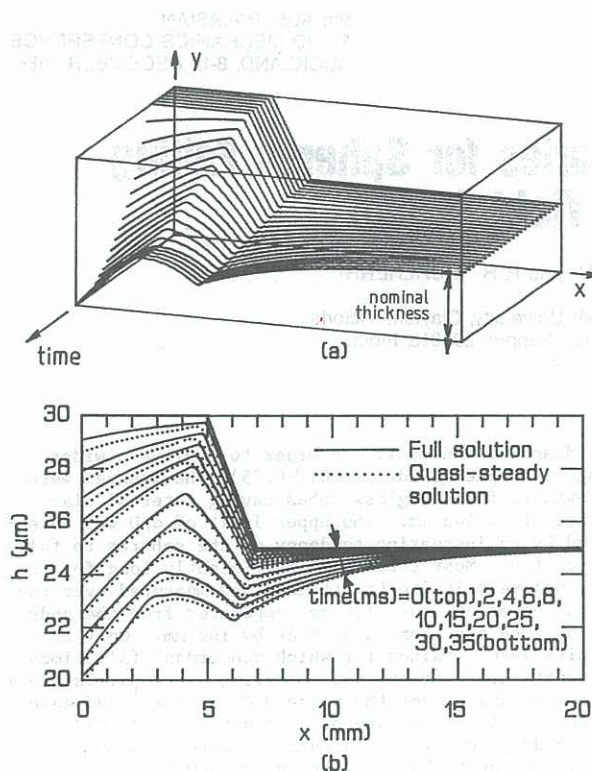


Figure 5 Variation of the film thicknesses,  $h$ , with time near the strip edge.

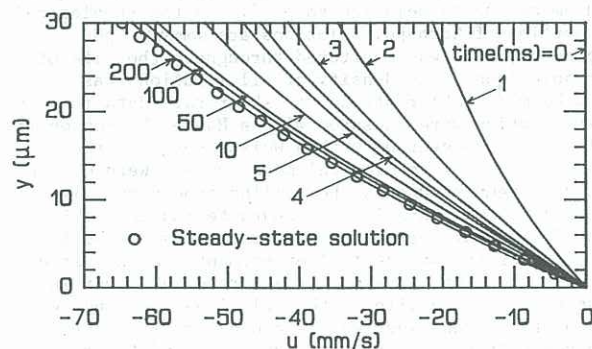


Figure 6 Variation of the film velocity,  $u$ , with time at  $x = 4$  mm.

device best suited for the specified operating conditions can be selected.

#### CONCLUSION

A solution for the flow of a thin film of viscous incompressible fluid subject to external pressure gradients and shear forces is presented. The analytical results have been applied to examine the effectiveness in the removal of the edge build-up defect by suction devices in a continuous strip

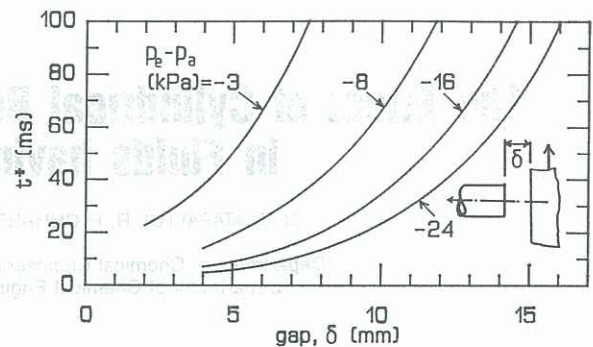


Figure 7 Suction time,  $t^*$ , required to eliminate the edge build-up for various suction tube entry pressures,  $P_e$ .

coating process.

#### REFERENCES

- Butler, J.J.; Beam, D.J.; Hawkins, J.C. (1970): The development of air coating control for continuous strip galvanizing. *Iron and Steel Engineer*, February, 77-86.
- Ellen, C.H.; Tu, C.V. (1983): An analysis of jet stripping of molten metallic coatings. *Proc. of the 8th Australasian Fluid Mechanics Conference*, 2C.4-2C.7, University of Newcastle, NSW.
- Ellen, C.H.; Tu, C.V. (1984): An analysis of jet stripping of liquid coatings. *Journal of Fluids Engineering*, Vol. 106, 399-404.
- Nikoleizig, A.; Kootz, T.; Weber, F.; Espenhahn, M. (1978): Fundamentals of the jet process for hot-dip galvanizing. *Stahl u Eisen*, Vol. 98, No. 7, 336-342 [in German].
- Pai, B.R.; Whitelaw, J.H. (1969): Simplification of razor blade technique and its application to the measurement of wall shear stress in wall jet flows. *Aero. Quarterly*, November, 355-364.
- Patel, V.C. (1965): Calibration of the Preston tube and limitations on its use in pressure gradients. *Journal of Fluid Mechanics*, Vol. 23, 185-208.
- Savage, M.D. (1982): Mathematical models for coating process. *Journal of Fluid Mechanics*, Vol. 117, 443-455.
- Thornton, J.A.; Graff, H.F. (1976): An analytical description of the jet finishing process for hot-dip metallic coatings on strip. *Metallurgical Transactions B*, Vol. 7B, December, 607-618.

#### ACKNOWLEDGEMENTS

The authors wish to thank the management of BHP Steel International Group, Coated Products Division, for permission to publish the information contained in this paper.